Curvature and confinement effects for flame speed measurements in laminar spherical and cylindrical flames.

Adrien Bonhomme, Laurent Selle, Thierry Poinsot

Curvature and confinement effects for flame speed measurements in laminar spherical and cylindrical flames

Adrien Bonhomme [a,*], Laurent Selle [a,b], Thierry Poinsot [a,b]

[a] Université de Toulouse, INPT, UPS, IMFT (Institut de Mécanique des Fluides de Toulouse), Allée Camille Soula, F-31400 Toulouse, France
[b] CNRS, IMFT, F-31400 Toulouse, France

A B S T R A C T

This paper discusses methods used to obtain laminar flame speeds in spherical laminar premixed flames. Most recent studies express the laminar flame consumption speed as $\rho_b/\rho_u\ dR/dt$, where R is the flame radius and ρ_b/ρ_u is the ratio of the burnt to the fresh gas density (ρ_b is evaluated at chemical equilibrium and supposed to be constant). This paper investigates the validity of this assumption by reconsidering it in a more general framework. Other formulae are derived and tested on a DNS of cylindrical flames (methane/air and octane/air). Results show that curvature and confinement effects lead to variations of ρ_b and ρ_u and to significant errors on the flame speed. Another expression (first proposed by Bradley and Mitcheson in 1976) is derived where no density evaluation is required and only pressure and flame radius evolution are used. It is shown to provide more precise results for the consumption speed than $\rho_b/\rho_u\ dR/dt$ because it takes into account curvature and confinement of the flame in the closed bomb.

Keywords:
Flame speed
Curvature
Confinement

1. Introduction

The experimental determination of the laminar consumption flame speed, s_L^0, is an overarching problem in combustion [1]. Indeed the knowledge of the rate at which the fresh gases are consumed is instrumental in the study of flame dynamics as well as the development of kinetic schemes. For modeling purposes, the laminar flame speed is the central ingredient of most turbulent-combustion models [2–6].

Despite the apparent simplicity in the formulation of the problem, measuring accurately s_L^0 is a delicate task. Since the early attempts, which date as far back as a hundred and fifty years ago [7–11], a variety of methods have been devised. These methods find their roots in analytical solutions of reacting fluid mechanics but most of them suffer from approximations or experimental difficulties that strongly affect their precision. For example, the flat flame propagating in a tube is strongly perturbed by instabilities or the presence of walls [12,13]. Other techniques require extrapolation or correcting factors in order to account for the effects of curvature or strain [14–17].

In the present paper, we revisit the classical technique of the '*spherical flame in a bomb*' (Fig. 1a): in a closed vessel, a mixture of fresh gases is ignited, a spherical flame develops and its radius, $R(t)$, is measured vs. time using simple optical methods.

Such experiments are fairly easy to conduct. Moreover initial conditions (temperature, pressure, composition, etc.) are well controlled and can be extended to high temperatures and pressures.

However, extracting flame speed values from spherical flames is a much more difficult exercise which has lead to multiple controversies in the past [18–22]. Two quantities can be measured experimentally to construct a flame speed in a bomb: (1) the flame radius evolution $R(t)$ and (2) the bomb pressure $P(t)$. Most existing methods use one of these two quantities (or the two) to deduce flame speeds.[1]

Assuming that $R(t)$ and/or $P(t)$ are available, two independent steps are then required to obtain flame speeds:

- STEP I: the instantaneous flame speed must be obtained from $R(t)$ and/or $P(t)$.
- STEP II: since a spherical flame is a stretched flame, the speed which is measured in STEP I is not the unstretched laminar flame speed s_L^0 but a stretched flame speed $s_L(\kappa)$ where $\kappa = 2/R\ dR/dt$ is the instantaneous flame stretch. Therefore a model for $s_L(\kappa)$ is needed to obtain s_L^0. This model is usually based on a Markstein-type correlation [21,24,25], for example the linear expression:

$$s_L(\kappa) = s_L^0 - \mathcal{L}\kappa \tag{1}$$

* Corresponding author.
E-mail addresses: adrien.bonhomme@imft.fr (A. Bonhomme), laurent.selle@imft.fr (L. Selle), thierry.poinsot@imft.fr (T. Poinsot).

[1] Recent methods using direct flow and front speed measurements have begun in the last two years [23] but they are not discussed here.

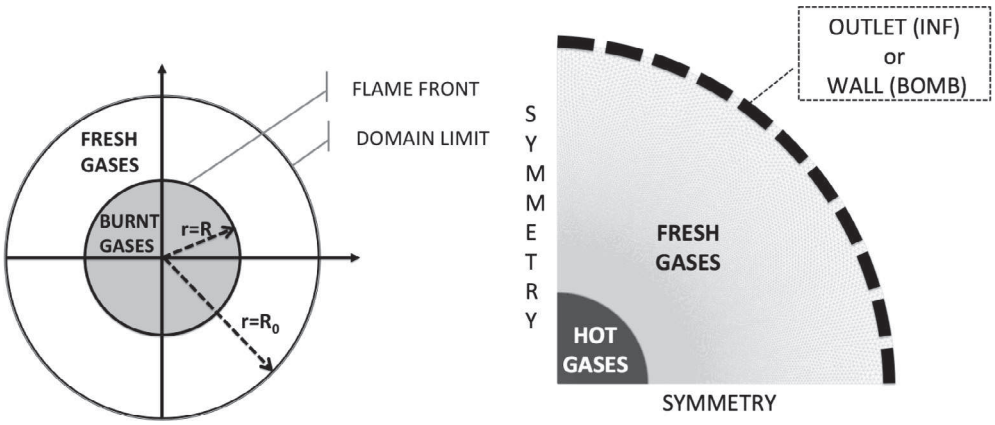

(a) Generic configuration for a spherical flame in a bomb.

(b) Computational domain for the cylindrical flame.

Fig. 1. Configuration for expanding flames.

where $\mathcal{L}$ is the Markstein length which becomes an additional unknown quantity to determine [26]. In the past five years, other expressions have also been proposed to replace Eq. (1) (mostly based on the non-linear form of s_b [27,21]).

This paper does not discuss STEP II and focuses on STEP I. During this step, approximations between the various flame speeds characterizing a front are utilized and the present work shows that they can have a direct impact on the result. Indeed, the only speed which is unambiguously measured in a bomb is the flame speed of the front relative to the burnt gases $s_b(\kappa) = dR/dt$ because the burned gases do not move.

Obtaining a relation between $s_b(\kappa)$ and $s_L(\kappa)$ is a delicate task because it requires well chosen assumptions. A classical, albeit approximate, relation used in multiple recent studies is:

$$s_L(\kappa) = \frac{\rho_b}{\rho_u} s_b(\kappa) \tag{2}$$

where ρ_b is the density of the burnt gases and ρ_u that of the unburnt gases.

In addition to stretch, other factors modify the flame speed in a spherical explosion [27,21,28,29]:

1. In the early stages, the energy of the spark modifies the burnt gases temperature as well as the flame speed.
2. Curvature effects and preferential diffusion (for non-unity Lewis number) also influence the evolution of the flame and the burnt gases temperature. In Eq. (2), most authors recognize that s_b depends on stretch but neglect the influence of stretch on ρ_b. However, the burnt gases density, like the burnt gases temperature, is affected by stretch too. And even if this effect is smaller than the effect of κ on s_L it must be taken into account.
3. For large radii, the confinement of the flame in a closed vessel influences ρ_u and ρ_b and therefore changes the flame speed.

The objective of the present work is to revisit the formulation of Eq. (2) and to propose theoretical expressions for the consumption flame speed that alleviate the problems of Eq. (2). The derivations are presented in Section 2 and Direct Numerical Simulations (DNS) are conducted in Section 3 where the formulae can be compared to the true consumption speed based on the integral of the reaction rate [6] in the case of a cylindrical flame. All derivations are performed in two cases: (1) INF where the flame propagates in an infinite medium, confinement effects do not exist and curvature effects due to non-unity Lewis number can be isolated, and (2) BOMB where the flame propagates in a closed bomb where both curvature and confinement affect the burnt and fresh gases density.

2. Theoretical results

Deriving an expression for flame speeds in a spherical or cylindrical flame (cf. Fig. 1a) is a complex exercise [27,30–32]. It is presented here without invoking an infinitely-thin-flame assumption. The formulae for the consumption flame speed presented in this paper are based on the conservation equation for the species. The definition of the consumption flame speed in a spherical flame is obtained from the integral of the reaction rate $\dot{\omega}_k$ of one specie k (fuel or products for example):

$$s_c = \frac{1}{\rho_u \left(Y_k^b - Y_k^u\right) R^2} \int_0^{R_0} \dot{\omega}_k r^2 dr \tag{3}$$

where ρ_u is the fresh gases density, Y_k^u and Y_k^b are the mass fraction of specie k in the fresh and burnt gases respectively and R_0 is the integration boundary[2] ($R_0 > R$). Since $\dot{\omega}_k$ cannot be measured experimentally, other indirect expressions are required for s_c. They can be derived by starting from the conservation equation of specie k [6]:

$$\frac{\partial \rho Y_k}{\partial t} + \vec{\nabla}(\rho(\mathbf{u} + \mathbf{V_k})Y_k) = \dot{\omega}_k \tag{4}$$

where Y_k is the mass fraction and $\mathbf{V_k}$ is the diffusion velocity of specie k. Integrating Eq. (4) over the control volume ($0 \leqslant r \leqslant R_0$) yields:

$$\frac{dM_k}{dt} + 4\pi R_0^2 \rho_u Y_k(r = R_0)[u_r(r = R_0) + V_{k,r}(r = R_0)] = \int_0^{R_0} \dot{\omega}_k 4\pi r^2 dr \tag{5}$$

where M_k is the total mass of specie k in the domain: $M_k = \int_V \rho Y_k dV$. The second left hand side term represent the flux of specie k leaving the domain at $r = R_0$. Including the definition of the flame speed s_c (Eq. (3)) in Eq. (5) gives:

$$\frac{dM_k}{dt} + 4\pi R_0^2 \rho_u Y_k(r = R_0)[u_r(r = R_0) + V_{k,r}(r = R_0)] = s_c 4\pi R^2 \rho_u \left[Y_k^b - Y_k^u\right] \tag{6}$$

[2] R_0 goes to the infinity for the case of a flame propagating in an infinte medium.

To obtain an explicit relation linking s_c to R, the second left hand side term in Eq. (6) must be canceled. So the optimal choice of the specie k depends on the configuration:

- In a hypothetical infinite medium (INF configuration) $u_r(r = R_0) > 0$. But if a product is used ($Y_p(r = R_0) = 0$), as long as the flame has not reached the position $r = R_0$ the second term on the LHS of Eq. (6) is also canceled.
- In a closed vessel (BOMB configuration) $u_r(r = R_0) = 0$ and $V_{k,r}(r = R_0) = 0$, so that any species can be used in Eq. (6).

At this point in the derivation a consumption speed has been defined but no assumptions were made. The idea is now to link M_k to the flame radius R in order to get an expression for s_c that is accessible to experimental measurements. Two cases are distinguished depending on which species k is used:

1. **A product** ($k = p$): a flame radius R_p based on the mass of products is defined as:

$$R_p^3 = \frac{M_p}{\frac{4\pi}{3}\overline{\rho_b} Y_{p,b}} \tag{7}$$

where $Y_{p,b}$ is the mass fraction of the product (e.g. CO_2) in the burnt gases and $\overline{\rho_b}$ is the burnt gases density (averaged spatially between $r = 0$ and $r = R_p$). Eq. (7) does not imply that the flame is thin: the mass of products M_p is defined unambiguously and R_p is the 'equivalent' radius of a sphere containing this mass. Combining Eqs. (6) and (7) to eliminate M_p yields:

$$s_c^p = \frac{\overline{\rho_b}}{\rho_u}\frac{dR_p}{dt} + \frac{R_p}{3\rho_u}\frac{d\overline{\rho_b}}{dt} \tag{8}$$

where the product mass fraction $Y_{p,b}$ is supposed to be constant. Eq. (8) is derived without assumptions on the domain where the flame propagates: it can be used in a bomb of any size or in an infinite domain [33].
In a simulation Eq. (8) can be used directly because $\overline{\rho_b}$, ρ_u and R_p can be measured. In an experiment, however, assumptions on $\overline{\rho_b}$ and ρ_u are required. The most usual is to suppose that densities are constant (in space and time). Thus, it is generally assumed than ρ_u remains equal to its initial value (neglecting confinement effects, as expected if the bomb is sufficiently large). And $\overline{\rho_b}$ is obtained by assuming that its value does not vary with r from 0 to R_p and is equal to the burnt gases density at equilibrium ρ_b^{eq} so that Eq. (8) leads to:

$$s_c^{p,expe} = \frac{\rho_b^{eq}}{\rho_u(t=0)}\frac{dR_p}{dt} \tag{9}$$

which is the expression used in most studies.[3]

2. **The fuel** ($k = f$): in an infinite domain, fuel cannot be used in Eq. (6) because its flux is not zero at $r = R_0$. However, in a bomb where $\mathbf{u}(r = R_0) = 0$ and $\mathbf{V_k}(r = R_0) = 0$, fuel can be used in Eq. (6) leading to a formulation given by [34]. In this case, the radius of the flame based on the mass of fuel is defined by[4]:

$$R_f^3 = R_0^3 - \frac{M_f}{\frac{4\pi}{3}\rho_u Y_{f,u}} \tag{10}$$

where $Y_{f,u}$ is the mass fraction of the fuel in the unburnt gases, which is constant. Combining Eqs. (6) and (10) yields:

$$s_c^f = \frac{dR_f}{dt} - \frac{R_0^3 - R_f^3}{3R_f^2}\frac{1}{\rho_u}\frac{d\rho_u}{dt} \tag{11}$$

Assuming an isentropic compression for the fresh gases which is a very reasonable approximation here, one has $(1/\rho_u)\, d\rho_u/dt = 1/(\gamma_u P)\, dP/dt$, where γ_u is the ratio of the heat capacities in the fresh gases. Eq. (11) is then recast into:

$$s_c^f = \frac{dR_f}{dt} - \frac{R_0^3 - R_f^3}{3R_f^2}\frac{1}{\gamma_u P}\frac{dP}{dt} \tag{12}$$

Note that Eqs. (9) and (12) are very different: Eq. (12) includes no density ratio in front of dR_f/dt which suggests that the pressure term dP/dt is important. Both expressions use a flame radius which is defined differently. For Eq. (9), the flame radius R_p is defined from the mass of products while for Eq. (12), the flame radius R_f is obtained from the mass of fuel. In practice, experimentally, the flame fronts are thin and it is probably impossible to distinguish R_p and R_f which are both equal to the observed flame radius R. In other words, an infinite thin flame assumption is implicitly done when post processing experiments. Eq. (12) can be used in bombs but not in an infinite medium. It has been previously derived [31,30,34] but it does not seem to be used, even though it is directly accessible in an experiment because it requires only R_f and P vs. time as input data. It will be shown in Section 3.4 using DNS that Eq. (12) is insensitive to curvature and confinement effects, unlike Eq. (9).

3. Validation with numerical simulations

All flame speed expressions derived in Section 2 are summarized in Table 1. To check their accuracy, Eqs. (8), (9) and (12) are compared here in a simulation of cylindrical flames with the true consumption flame speed s_c defined by Eq. (3).

Direct Numerical Simulations of cylindrical flames are performed using the AVBP code [35]. AVBP is an unsteady compressible Navier–Stokes solver. The present simulations are performed with a third-order (in space and time) scheme called TTGC [36]. In order to address both confinement and Lewis number effects, two simulations with different fuels in air are conducted: a lean methane/air ($Le_{CH_4} = 0.996,\ \Phi = 0.8$) flame and a lean octane/air flame ($Le_{C_8H_{18}} = 2.78,\ \Phi = 0.8$). The Lewis number is defined by $Le_k = D_{th}/D_k$, where $D_{th} = \lambda/(\rho c_p)$ is the heat diffusivity coefficient and D_k is the diffusion coefficient of specie k in the mixture. Moreover two geometrical cases are also compared (configuration INF and BOMB).

3.1. Kinetic schemes

Reduced two-step mechanisms are used for this work:

1. For methane a scheme [37] called 2S_CH4_CM2 is employed.

$$CH_4 + \frac{3}{2}\ O_2 \rightarrow CO + 2\ H_2O \tag{13}$$

$$CO + \frac{1}{2}\ O_2 \leftrightarrow CO_2 \tag{14}$$

2. For octane, a scheme called 2S_C8H18_AB was developed following the same methodology.

$$C_8H_{18} + \frac{17}{2}\ O_2 \rightarrow 8\ CO + 9\ H_2O \tag{15}$$

$$CO + \frac{1}{2}\ O_2 \leftrightarrow CO_2 \tag{16}$$

[3] Note that an intermediate formulation could be $s_c^{p,expe,2} = \overline{\rho_b}/\rho_u dR_p/dt$ if a good approximation can be found for $\overline{\rho_b}$. We tested this solution but it shows that in Eq. (8) a good evaluation of both $\overline{\rho_b}$ and $d\overline{\rho_b}/dt$ is important. In practice, even if this solution had worked in the DNS where we can have access to ρ_b, it would have been difficult to use in an experiment since ρ_b is hardly measurable. $s_c^{p,expe,2}$ is not discuss anymore in this work.

[4] The present derivation is valid for lean flames and is based on the fuel balance. For rich flames, a similar derivation based on oxygen leads exactly to the same expression.

Table 1
Consumption flame speed expressions in laminar deflagrations. R_0 is the radius of the spherical bomb. R, R_p and R_f are evaluations of the flame radius. ρ_b^{eq} is the burnt gases density at equilibrium.

Symbol	Name	Expression	Validity
s_c	True consumption speed	$s_c = \frac{1}{\rho_u(Y_k^b - Y_k^u)R^2}\int_0^{R_0} \dot{\omega}_k r^2 dr$	Definition
s_c^p	Speed based on conservation of burnt gases	$s_c^p = \frac{\overline{\rho_b}}{\rho_u}\frac{dR_p}{dt} + \frac{R_p}{3\rho_u}\frac{d\overline{\rho_b}}{dt}$	Bombs or infinite medium
$s_c^{p,expe}$	Speed based on conservation of burnt gases & constant densities assumption	$s_c^{p,expe} = \frac{\rho_b^{eq}}{\rho_u(t=0)}\frac{dR_p}{dt}$	Bombs of very large size or infinite medium
s_c^f	Speed based on fuel conservation	$s_c^f = \frac{dR_f}{dt} - \frac{R_0^3 - R_f^3}{3R_f^2}\frac{1}{\gamma_u P}\frac{dP}{dt}$	Bombs only (of any size)

Both schemes account for the oxidation of the fuel through an irreversible reaction at a rate q_1 while a second reaction accounts for the equilibrium between CO and CO_2 with a rate q_2:

$$q_1 = A_1\left(\frac{\rho Y_F}{W_F}\right)^{n_1^F}\left(\frac{\rho Y_{O_2}}{W_{O_2}}\right)^{n_1^{O_2}} exp\left(\frac{E_{a,1}}{RT}\right) \quad (17)$$

$$q_2 = A_2\left[\left(\frac{\rho Y_{CO}}{W_{CO}}\right)^{n_2^{CO}}\left(\frac{\rho Y_{O_2}}{W_{O_2}}\right)^{n_2^{O_2}} - \frac{1}{K_e}\left(\frac{\rho Y_{CO_2}}{W_{CO_2}}\right)^{n_2^{CO_2}}\right] exp\left(\frac{E_{a2}}{RT}\right) \quad (18)$$

where K_e is the equilibrium constant for the CO/CO_2 equilibrium and R the perfect-gas constant. The coefficients for the two schemes are recalled in Table 2.

While the reduced scheme for methane has already been validated [37], the validation of the 2S_C8H18_AB scheme for octane vs. a detailed scheme [38] is presented in Fig. 2.

For a one-dimensional planar flame at $P_0 = 101{,}325$ Pa and $T_0 = 323$ K, the reduced scheme reproduces accurately the laminar flame speed and burnt gases adiabatic temperature, for equivalence ratios up $\Phi = 1.2$.

3.2. Numerical set-up

The definition of the consumption speed, given in Eq. (3), cannot be measured in an experiment but it can easily be computed from a DNS: this is how the formulae proposed in this paper (Eqs. (8) and (12)) as well as the approximation of Eq. (9) are validated. A cylindrical flame propagating in a domain of size $R_0 = 10$ cm is considered (Fig. 1b). When non-reflecting boundary conditions [39] are used at $r = R_0$, the configuration mimics an infinite medium where pressure is constant (INF configuration). If a wall is setup at $r = R_0$, the configuration corresponds to a closed vessel (BOMB configuration). Table 3 summarizes these two configurations.

Using symmetry boundary conditions, only a quarter of the bomb is meshed. The grid is refined within a radius $r < 30$ mm from the center with a cell size $\Delta = 25$ μm to ensure that the flame front is fully resolved: 17–20 points in the thermal flame thickness, defined by $\delta_l^0 = (T_b - T_u)/\max dT/dr$ ($\delta_l^0 = 0.43$ mm for octane and 0.51 mm for methane). The thermodynamic conditions for all simulations presented in this paper are $\Phi = 0.8$, $P_0 = 101{,}325$ Pa and $T_0 = 323$ K. As suggested by Bradley [33], the time interval used for plots corresponds to phases where the flame has grown enough ($R > 5.5$ mm) to have forgotten initial conditions but is still small enough compared to the size of the bomb ($R < 26.5$ mm) to avoid wall effects and remain perfectly spherical. The flame is initialized by introducing a sphere of burnt gases of radius 1 mm, at temperature, density and species mass fractions corresponding to the equilibrium conditions. This avoids to considers the details of the ignition phase and corresponds to the assumptions required for Eq. (9).

Table 2
Coefficients for the reduced kinetic schemes. Activation energies are in [cal mol^{-1}] and pre-exponential constants in [cgs] units

q_1	A_1	$E_{a,1}$	n_1^F	$n_1^{O_2}$	
methane	2.00×10^{15}	35,000	0.9	1.1	
octane	6.05×10^{11}	41,500	0.55	0.9	
q_2	A_2	$E_{a,2}$	n_2^{CO}	$n_2^{O_2}$	$n_2^{CO_2}$
methane	2.00×10^{9}	12,000	1.0	0.5	1.0
octane	4.50×10^{10}	20,000	1.0	0.5	1.0

3.3. Curvature effects only: cylindrical flame in an infinite medium

First, numerical simulations are performed in an idealized case (INF configuration) where there is no compression to study the impact of the curvature effects only. This is achieved by using a non-reflecting outlet boundary condition (cf. Fig. 1b) at $r = R_0$. Thus, pressure, fresh-gases temperature and density remain constant. In this configuration, there is a flux of fresh gases through the boundary $r = R_0$ so that Eq. (8), based on the conservation of the product species is used. Eq. (12) cannot be used in the INF configuration.

Consequently, Fig. 3 presents the comparison of Eqs. (8) and (9) with the true consumption flame speed s_c (Eq. (3)) for both fuels.

Eq. (8) matches the true consumption speed for both fuels. Moreover all curves extrapolate to s_L^0 at $\kappa = 0$. Interestingly, Eq. (9) shows a different behavior for the two fuels: while for methane it matches the true consumption speed, except in the very early times, for octane, there is a clear gap between the two curves. In other words, Eq. (9) does not predict the correct stretched flame speed for the octane/air flame. This phenomenon is due to a Lewis number effect. When the flame is stretched, the burnt gases temperature is not equal to the adiabatic burnt gases temperature T_{ad}. Figure 4 displays various temperature profiles vs. radius r when the octane/air flame propagates. Shortly after the ignition, the maximum temperature drops from the equilibrium $T_{ad} = 2051$ - K to about 1840 K. When the flame propagates, the temperature goes up again and comes back to T_{ad} at the end of the simulation.

These changes are due to stretch: like the flame speed, the adiabatic flame temperature is influenced by stretch and this effect has been analyzed in the literature [40,41]. The relation between the burnt gases temperature T_b and stretch κ is:

$$\frac{T_b - T_{ad}}{T_{ad}} = \left(\frac{1}{Le} - 1\right)\frac{D}{s_L^{0^2}}\kappa \quad (19)$$

where Le is the Lewis number of the limiting reactant and D a characteristic diffusivity. For the methane/air flame since $Le_{CH4} = 0.996$, T_b is almost insensitive to stretch so that $\overline{\rho_b}$ is close to its equilibrium value and Eq. (9) is close to the true flame speed (Fig. 3b). On the other hand, for octane ($Le_{C8H18} = 2.78$), $T_b < T_{ad}$ so that $\overline{\rho_b} > \rho_b^{ad}$ leading to an underestimation of $s_c(\kappa)$ in Fig. 3a by 2–3%. To compare Eq. (19) and simulations, a temperature that represents

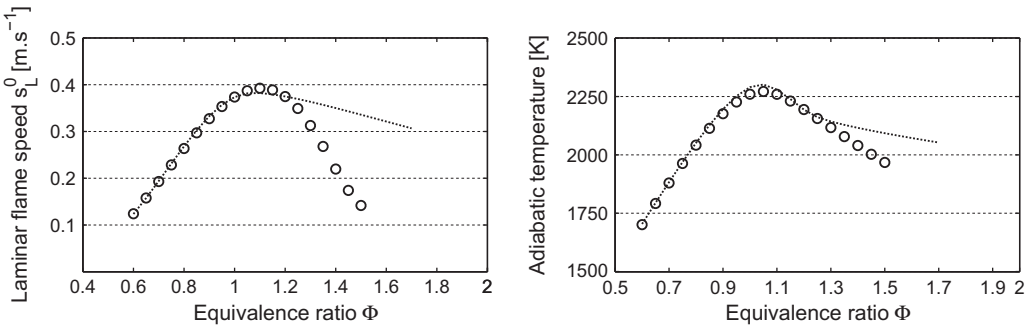

(a) Laminar flame speed. (b) Adiabatic temperature.

Fig. 2. Validation of the reduced scheme for octane/air flames at P_0 = 101,325 Pa and T_0 = 323 K. ○ Jerzembeck et al. [38], ……, 2S_C8H18_AB.

Table 3
Details on INF and BOMB configurations.

Case	Boundary conditions at $r = R_0$	Expression
INF	Non-reflecting	Infinite medium, constant pressure
BOMB	$\mathbf{u} = 0$	bomb of radius R_0, pressure goes up

fairly the burnt gases temperature for a given stretch must be defined. The maximum of temperature T_b^{max} seems to be reasonable here, as presented by Fig. 5. In this paper, the characteristic diffusivity D used is the fuel molecular diffusivity in the fresh gases D_f^u.

Figure 6 presents the comparison of Eq. (19) and results obtained in methane and octane air flame simulations.

A good agreement between theory and simulation is found: it confirms that the burnt gases temperature (and therefore the burnt gases density in Eq. (9)) are not constant and change with stretch if the Lewis number is not equal to unity. Figure 6 shows that for

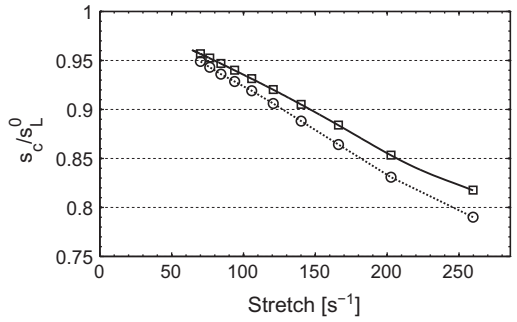

(a) Octane.

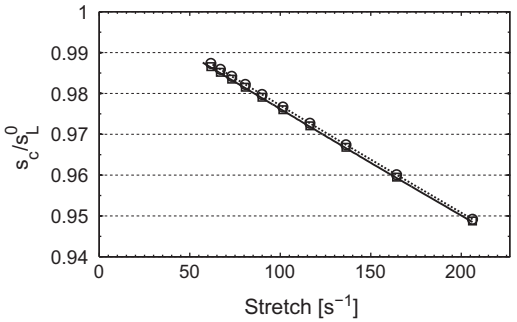

(b) Methane.

Fig. 3. Normalized consumption speed vs. stretch for a configuration without compression (INF) with $s_L^{0,CH4} = 0.255$ m/s and $s_L^{0,C8H18} = 0.264$ m/s: — s_c (Eq. (3)); -⊖- $s_c^{p,expe}$ (Eq. (9)); □ s_c^p (Eq. (8)).

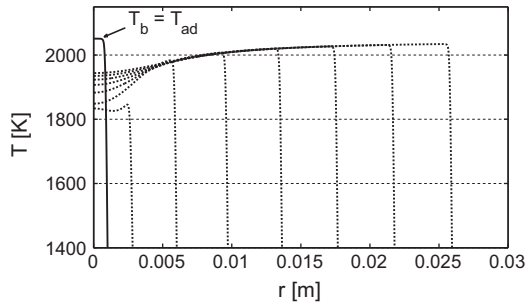

Fig. 4. Temperature profiles vs. the flame radius R when the octane/air flame propagates. — Initial solution ($T_b = T_{ad}$); ---- Temporal evolution: time varies from $t = 0$ to $t = 17.5$ ms by step of 2.5 ms.

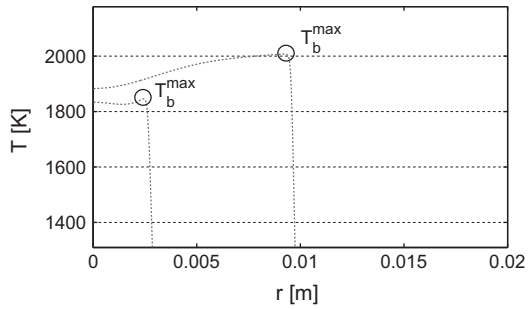

Fig. 5. Definition of T_b^{max} with the temperature profiles vs. the flame radius r.

methane, Lewis effects are neglectible but not for octane. This explains why in Fig. 3, $s_c^{p,expe}$ matches the true consumption flame speed s_c for the methane but not for the octane.

3.4. Combined curvature and confinement effects: cylindrical flame in a closed bomb

Figure 7 shows the evolution of the various expressions for the consumption speed,[5] normalized by the unstretched laminar flame speed s_L^0, vs. stretch. Using Eq. (9) (open circles) one recovers the classical shape for the flame speed: fairly linear at high stretch (small radii) but bent downward for lower stretch (large radii). However, the true consumption speed based on the integral of the fuel

[5] Eqs. (8) and (12) are derived for a spherical flame but it is straightforward to modify them for a cylindrical flame. In this case Eq. (8) becomes $s_c^p = \frac{\overline{\rho_b}}{\rho_u}\frac{dR_p}{dt} + \frac{R_p}{2\rho_u}\frac{d\overline{\rho_b}}{dt}$ and Eq. (12) becomes $s_c^f = \frac{dR_f}{dt} - \frac{R_0^2 - R_f^2}{2R_f}\frac{1}{\gamma_u P}\frac{dP}{dt}$.

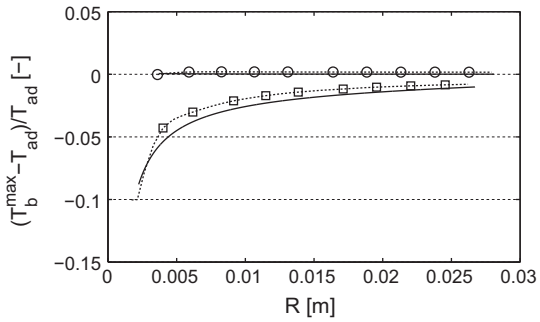

Fig. 6. Normalized burnt gases temperature $(T_b^{max} - T_{ad})/T_{ad}$ vs. the flame radius R. -□- C8H18; -○- CH4; — Theoretical expression of Clavin and Williams (Eq. (19)).

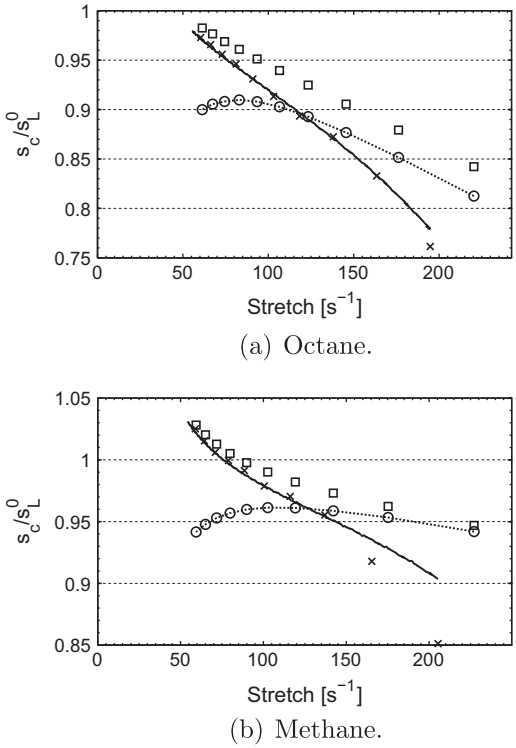

Fig. 7. Normalized consumption speed vs. stretch in a closed bomb (BOMB) with $s_L^{0,CH4} = 0.255$ m/s and $s_L^{0,C8H18} = 0.264$ m/s: — s_c (Eq. (3)); -○- $s_c^{p,expe}$ (Eq. (9)); □ s_c^p (Eq. (8)); ×s_c^f (Eq. (12)).

consumption rate (Eq. (3), solid line in Fig. 7) does not show a reduction as the flame grows. In the present configuration, for $\kappa < 150$ s^{-1}, the departure between Eqs. (3) and (9) is significant ($\simeq$8% at low stretch).

The reason why Eq. (9) is not right here is that Eq. (9) uses the approximation $\overline{\rho_b} = \rho_{ad}$. Figure 8 displays the time variation of $\overline{\rho_b}$ is the BOMB case for octane and methane. As expected:

- for methane, at small times, curvature effects have no influence on $\overline{\rho_b}$. At later times, curvature effects decrease but confinement effects appear: pressure goes up and so does $\overline{\rho_b}$, an effect which is ignored by Eq. (9).
- for octane flames the situation is not better: curvature effects lead to an increase of $\overline{\rho_b}$ at small times and confinement effects only make it worse at later times.

The standard procedure with such data is to extrapolate the linear portion of the curve towards $\kappa = 0$. As illustrated in [27] (their

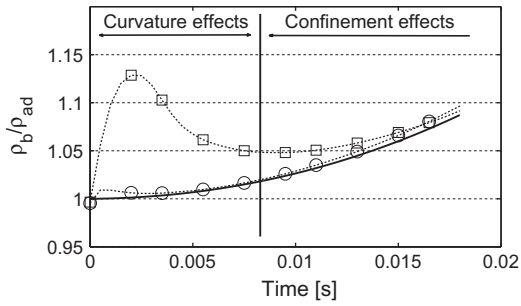

Fig. 8. Normalized burnt gases density $\overline{\rho_b}/\rho_{ad}$ vs. time. -□- C8H18; -○- CH4; — isentropic compression ($P/\overline{\rho_b}^{\gamma_b} = $ cste).

Fig. 5), the length of this linear portion is greatly influenced by the size of the apparatus, i.e. by confinement. This sensitivity affects the precision of the extrapolation procedure, as shown in [29] using both linear and non-linear methods. However, the consumption speed s_c^p (Eq. (8), open squares in Fig. 7) does not match exactly the true consumption flame speed s_c (Eq. (3)) at large stretch. This can be explained by the difference between R_f and R_p, especially when the flame is very small. Indeed, replacing R_p by R_f in Eq. (8) leads to a better result. In practice, s_c^p is not used in an experiment because $d\rho_b/dt$ is not easily accessible. Conversely, the consumption speed s_c^f based on the conservation of the fuel (Eq. (12)) is easy to measure and is unaffected by the confinement as shown in Fig. 7. This expression matches perfectly the true consumption flame speed s_c.

For methane, in the early development of the flame $\kappa > 150$ s^{-1}, s_c^f does not seem to match well the true consumption speed because the pressure increase is very small initially. At later times (the region in which we are interested and where stretch is smaller) the accuracy of Eq. (12) is very good.

Note that the simulations of Sections 3.3 and 3.4 were conducted in a 2D configuration. In a cylindrical flame, the pressure increase is much stronger than for a spherical flame so that confinement effects are overestimated in the present simulations. The first consequence is that for a spherical bomb with the same radius R_0, the diminution of s_L at low stretch would be less pronounced. Nevertheless, even with an exaggerated pressure increase, Eq. (12) is more precise than the classical formulae, which can only improve the accuracy of the extrapolation method. The second consequence is that even at moderate flame radii, the pressure and temperature increase in the fresh gases changes the flame speed. This is particularly striking for the methane flame in Fig. 7b as the normalized consumption flame speed exceeds unity at $\kappa < 70$ s^{-1} because the fresh gases are not in the nominal conditions any more. This peculiarity of the cylindrical flame does not affect the conclusion about the precision of Eq. (12) vs. Eq. (9).

4. Conclusion

This study addresses the issue of post-processing flame radii, obtained from spherical flames in bombs, to deduce laminar flame speeds and Markstein lengths. These experiments raise difficult questions [27]: when the flame is too small, it is influenced by curvature and non-unity Lewis number effects; when it is too large, it is affected by the confinement effect of the bomb. In the present work, the limitations of the classical formula used experimentally to construct flame speeds from flame radius measurements ($s_L = \rho_b/\rho_u\, dR/dt$) are discussed.

Two expressions for the consumption speed were derived from the conservation equation of the species, without the assumption of an infinitely-thin flame front. The first one (Eq. (8)) is the generalization of the classical formula that accounts for the temporal

evolution of the density in the fresh and burnt gases. Because this formula requires the mean burnt gases density as an input, a quantity which cannot be measured in experiments, another expression (Eq. (12)) using only the flame radius and the pressure inside the bomb (two quantities which are directly measured) is presented (existing in the literature [34] but seldom used).

A cylindrical flame computed with DNS was used to evaluate the precision of these two expressions for the consumption flame speed. In a configuration where confinement effects do not exist (propagation in an infinite medium where pressure is rigorously constant), Eq. (9) incorrectly predicts the flame speeds for non-unity Lewis number (octane) but performs correctly for methane because Lewis number is close to unity in this case. In a second configuration, corresponding to a bomb, results show that Eq. (9) incorrectly predicts flame speeds for both octane and methane/air flames because the burnt gases density increases with pressure (in addition to curvature effects for octane) while Eq. (12) captures the correct consumption speed. Since Eq. (12) only requires the knowledge of $R(t)$ and $P(t)$, it is simple to use experimentally and the present work suggests that it is a good candidate for a more precise determination of the flame speeds. The main difficulty of this method should be the measurement and treatment of the pressure signal because the pressure increase in a large bomb may be difficult to measure accurately and to post process to obtain the pressure derivative required in Eq. (12).

References

[1] E. Ranzi, A. Frassoldati, R. Grana, A. Cuoci, T. Faravelli, A. Kelley, C. Law, Prog. Energy Combust. Sci. 38 (4) (2012) 468–501.
[2] K.N.C. Bray, M. Champion, P.A. Libby, in: R. Borghi, S. Murthy (Eds.), Turbulent Reactive Flows, Lecture Notes in Engineering, vol. 40, Springer Verlag, 1989, pp. 541–563.
[3] S.B. Pope, Ann. Rev. Fluid Mech. (1994) 23–63.
[4] N. Peters, Turbulent Combustion, Cambridge University Press, 2001.
[5] D. Veynante, L. Vervisch, Prog. Energy Combust. Sci. 28 (2002) 193–266.
[6] T. Poinsot, D. Veynante, Theoretical and Numerical Combustion, third ed., 2011. <www.cerfacs.fr/elearning>.
[7] E. Mallard, H. Le Chatelier, Astron. Astrophys., Paris 93 (1881) 145.
[8] E. Mallard, H. Le Chatelier, Ann. Min. 4 (1883) 274.
[9] H. Le Chatelier, Lecons sur le carbone, la combustion, les lois chimiques, Hermann, 1907.
[10] R.V. Wheeler, J. Chem. Soc. 115 (1919) 81–94.
[11] P. Laffitte, La propagation des flammes dans les mélanges gazeux, Hermann et Cie, Actualités scientifiques et industrielles, Paris, 1939.
[12] G.I. Sivashinsky, Combust. Sci. Tech. 15 (1977) 137–146.
[13] P. Clavin, Proc. Combust. Inst. 28 (2000) 569–586.
[14] R.A. Strehlow, L.D. Savage, Combust. Flame 31 (1978) 209.
[15] S.M. Candel, T. Poinsot, Combust. Sci. Technol. 70 (1990) 1–15.
[16] F.A. Williams, Combustion Theory, Benjamin, Cummings, Menlo Park, CA, 1985.
[17] L. Selle, T. Poinsot, B. Ferret, Combust. Flame 158 (1) (2011) 146–154.
[18] M.I. Hassan, K.T. Aung, G.M. Faeth, Combust. Flame 115 (4) (1998) 539–550.
[19] D.R. Dowdy, D.B. Smith, S.C. Taylor, in: 23rd Symp. (Int.) Combust., The Combustion Institute., Pittsburgh, 1990, pp. 325–332.
[20] T. Poinsot, Combust. Flame 113 (1998) 279–284.
[21] F. Halter, T. Tahtouh, C. Mounaïm-Rousselle, Combust. Flame 157 (10) (2010) 1825–1832.
[22] K. Eisazadeh-Far, A. Moghaddas, J. Al-Mulki, H. Metghalchi, Proc. Combust. Inst. 33 (1) (2011) 1021–1027.
[23] E. Varea, V. Modica, A. Vandel, B. Renou, Combustion and Flame. 159 (2012) 577–590.
[24] J. Tien, M. Matalon, Combust. Flame 84 (3–4) (1991) 238–248.
[25] J.K. Bechtold, M. Matalon, Combust. Flame 127 (1–2) (2001) 1906–1913.
[26] H.G. Im, J.H. Chen, Int. Symp. Combust. 28 (2000) 1833–1840.
[27] A. Kelley, C. Law, Combust. Flame 156 (9) (2009) 1844–1851.
[28] Z. Chen, Combust. Flame 157 (12) (2010) 2267–2276.
[29] Z. Chen, Combust. Flame 158 (2) (2011) 291–300.
[30] D. Bradley, A. Mitcheson, Combust. Flame 32 (1978) 221–236.
[31] D. Bradley, A. Mitcheson, Combust. Flame 32 (1978) 237–255.
[32] A.P. Kelley, J.K. Bechtold, C.K. Law, in: 7th US National Technical Meeting of the Combustion Institute, 2011, pp. 1–24.
[33] D. Bradley, P.H. Gaskell, X.J. Gu, Combust. Flame 104 (1–2) (1996) 176–198.
[34] D. Bradley, A. Mitcheson, Combust. Flame 26 (1976) 201–217.
[35] N. Gourdain, L. Gicquel, G. Staffelbach, O. Vermorel, F. Duchaine, J.-F. Boussuge, T. Poinsot, Comput. Sci. Discovery 2 (1) (2009) 015004.
[36] O. Colin, M. Rudgyard, J. Comput. Phys. 162 (2) (2000) 338–371.
[37] L. Selle, G. Lartigue, T. Poinsot, R. Koch, K.-U. Schildmacher, W. Krebs, B. Prade, P. Kaufmann, D. Veynante, Combust. Flame 137 (4) (2004) 489–505.
[38] S. Jerzembeck, N. Peters, P. Pepiot-Desjardins, H. Pitsch, Combust. Flame 156 (2) (2009) 292–301.
[39] T. Poinsot, S. Lele, J. Comput. Phys. 101 (1) (1992) 104–129.
[40] C.K. Law, P. Cho, Int. Symp. Combust. (1986) 1803–1809.
[41] P. Clavin, F. Williams, J. Fluid Mech. 116 (1982) 251–282.